Genetic analysis of β1 integrin "activation motifs" in mice

Aleksandra Czuchra,[1] Hannelore Meyer,[1] Kyle R. Legate,[1] Cord Brakebusch,[2] and Reinhard Fässler[1]

[1]Max Planck Institute of Biochemistry, Department of Molecular Medicine, 82152 Martinsried, Germany
[2]University of Copenhagen, Department of Molecular Pathology, 2100 Copenhagen, Denmark

A key feature of integrins is their ability to regulate the affinity for ligands, a process termed integrin activation. The final step in integrin activation is talin binding to the NPXY motif of the integrin β cytoplasmic domains. Talin binding disrupts the salt bridge between the α/β tails, leading to tail separation and integrin activation. We analyzed mice in which we mutated the tyrosines of the β1 tail and the membrane-proximal aspartic acid required for the salt bridge. Tyrosine-to-alanine substitutions abolished β1 integrin functions and led to a β1 integrin–null phenotype in vivo. Surprisingly, neither the substitution of the tyrosines with phenylalanine nor the aspartic acid with alanine resulted in an obvious defect. These data suggest that the NPXY motifs of the β1 integrin tail are essential for β1 integrin function, whereas tyrosine phosphorylation and the membrane-proximal salt bridge between α and β1 tails have no apparent function under physiological conditions in vivo.

Introduction

Integrins are heterodimeric cell surface receptors, consisting of an α and a β subunit, which play an important role in cell migration and tissue integrity by mediating cell attachment to the surrounding ECM and to other cells (Brakebusch and Fässler, 2005). Integrins can adopt high- and low-affinity conformations, and ligand binding to integrins is preceded by intracellular changes, resulting in increased integrin affinity (inside-out signaling; Ginsberg et al., 2005). Tight regulation of integrin affinity is crucial for the physiological function of integrins. During inflammation, for example, leukocytes can only extravasate into the affected tissue after a chemokine-induced increase in integrin affinity (Sackstein, 2005). Similarly, blood clotting is restricted to wounds by efficient control of the affinity of platelet integrin (Bennett, 2005).

Although the molecular mechanisms controlling integrin-mediated adhesion by inside-out signaling are not well understood, much is known about the structural changes that occur during integrin activation (Arnaout et al., 2005). Crystal structure analysis suggests a bent, hooklike conformation of the extracellular domain for the inactive state and an extended conformation in the active, high-affinity state (Takagi and Springer, 2002). Recent three-dimensional EM structural analysis, however, demonstrates that the bent conformation of αvβ3 is also able to bind efficiently to ligands, at least in the presence of Mn^{2+}, indicating that Mn^{2+}-induced activation takes place through small local conformational changes and not by straightening the extracellular domain (Adair et al., 2005). Although all these studies were done with β3 integrins, the conclusions conceivably can be extended to β1 integrin because of the high extent of structural similarity.

Many lines of experimental evidence indicate that binding of talin to the cytoplasmic domain of β1 integrin is a final common step in integrin activation (Liddington and Ginsberg, 2002; Tadokoro et al., 2003). Talin is a rodlike molecule with a globular head domain, which links integrins to the actin cytoskeleton. It binds to the membrane-proximal NPXY motif of β1, β2, and β3 integrin via a phosphotyrosine binding–like region in the FERM domain of the talin head. This binding is suggested to disrupt a salt bridge between the α and β subunits, which is believed to keep the integrin in an inactive state (Vinogradova et al., 2002). In addition, specific van der Waals interactions between the transmembrane regions of the α and β subunits are supposedly altered after talin binding, leading to conformational changes that are propagated across the plasma membrane, resulting in integrin activation (Luo et al., 2004). Talin binding to integrin is promoted by proteolytic cleavage of talin and binding of phosphoinositol phosphates and may be regulated by phosphorylation of talin (Critchley, 2005). It was proposed that phosphorylation of the NPXY motif in the integrin β subunit interferes with integrin activation by talin

Correspondence to Reinhard Fässler: faessler@biochem.mpg.de

Abbreviations used in this paper: Col1, collagen I; Erk, extracellular signal–regulated kinase; ES, embryonic stem; FA, focal adhesion; FN, fibronectin; HE, hematoxylin-eosin; K5, keratin 5; KI, knock-in; LN5, laminin 5; P, postnatal day.

The online version of this article contains supplemental material.

The Journal of Cell Biology, Vol. 174, No. 6, September 11, 2006 889–899
http://www.jcb.org/cgi/doi/10.1083/jcb.200604060

in two different ways. First, tyrosine phosphorylation of the NPXY motif might reduce the affinity for talin to such an extent that talin can no longer bind the β subunit. Second, NPXY phosphorylation might increase the affinity for other phosphotyrosine binding domain–containing proteins, to competitively inhibit the interaction with talin (Calderwood, 2004). Indeed, tyrosine-phosphorylated β3 integrin preferably interacts with Shc and not with talin (Cowan et al., 2000).

Mutational studies support a negative regulation function of tyrosine phosphorylation on integrin activation. Fibroblastoid cells expressing a β1 integrin in which the tyrosines in both NPXY motifs were substituted with nonphosphorylatable phenylalanines (YY783/795FF) were able to more effectively bind and assemble fibronectin (FN), similar to β1 mutants in which formation of the salt bridge to the α subunit is prohibited (D759A; Sakai et al., 1998a). In addition, YY783/795FF mutants showed partially altered outside-in signaling characterized by defective FAK activation but normal p130Cas phosphorylation (Wennerberg et al., 2000). Transformation with v-src results in tyrosine phosphorylation of β1 integrin, correlating with decreased β1 integrin–mediated adhesion (Sakai et al., 2001). V-src did not induce decreased adhesion in the nonphosphorylatable YY783/795FF β1 mutant, suggesting that tyrosine phosphorylation of integrins inhibits integrin activation and contributes to cell transformation by v-src.

In this study, we investigated the mechanism of integrin activation under physiological conditions and generated mice in which we replaced endogenous β1 integrin by mutant forms of β1, lacking either the aspartic acid essential for the salt bridge with the α subunit (D759A) or the tyrosine residues of the two cytoplasmic NPXY motifs (YY783/795FF), thus preventing inactivation by tyrosine phosphorylation. Surprisingly, both mutations did not cause any obvious phenotype, indicating that neither the salt bridge nor the phosphorylation of the intracellular tyrosines of β1 integrin is important for the regulation of β1 integrin activation. Substitution of the tyrosines with alanines (YY783/795AA), however, completely abolished β1 integrin function, confirming the crucial role of the NPXY motifs for integrin activation.

Results

Generation of mice carrying point mutations in the cytoplasmic domain–encoding region of the β1 integrin gene

To study the role of amino acid residues and protein motifs important for integrin activation during mouse development as well as in adult tissues, we established several mouse strains with point mutations in the cytoplasmic domain of the β1A integrin subunit (Fig. 1). First, we tested the relevance of the membrane-proximal salt bridge between α and β1 subunits by exchanging the aspartic acid residue 759 to alanine (D759A [D/A]), which destroys the salt bridge. Second, we addressed the potential role of tyrosine phosphorylation of the two conserved NPXY motifs within the β1 cytoplasmic domain, the proximal of which was shown to recruit talin. To this end, we established mice in which one or both tyrosines were exchanged to the nonphosphorylatable phenylalanine (Y783F; Y795F; YY783/795FF [YY/FF]).

	exon 15	exon 16
β1A wt	KLLMIIHDRREFAKFEKEKMNAKWDT	GENPIYKSAVTTVVNPKYEGK
β1A D759A	KLLMIIHARREFAKFEKEKMNAKWDT	GENPIYKSAVTTVVNPKYEGK
β1A Y783F	KLLMIIHDRREFAKFEKEKMNAKWDT	GENPIFKSAVTTVVNPKYEGK
β1A Y795F	KLLMIIHDRREFAKFEKEKMNAKWDT	GENPIYKSAVTTVVNPKFEGK
β1A YY783/795FF	KLLMIIHDRREFAKFEKEKMNAKWDT	GENPIFKSAVTTVVNPKFEGK
β1A YY783/795AA	KLLMIIHDRREFAKFEKEKMNAKWDT	GENPIAKSAVTTVVNPKAEGK

Figure 1. **Amino acid alignment of the cytoplasmic regions of wild-type and mutant β1A integrin subunits.** Mutated residues are highlighted in red, and regions encoded by exons 15 and 16 are indicated by solid lines.

A nonconservative change of the NPXY motifs was achieved by replacing the tyrosines by alanine (YY783/795AA [YY/AA]).

All mutations were introduced by homologous recombination into embryonic stem (ES) cells (Fig. 2, A and B) and confirmed by sequence analysis (not depicted). Positive ES cell clones of each mutation were injected into blastocysts to establish the mutant knock-in (KI) mouse strains (KI^{neo+}; Fig. 2, A and B). The loxP-flanked neomycin gene was then removed by intercrossing the mutant mouse strains with a deleter-Cre strain, resulting in mice carrying an intronic loxP site and defined point mutations in the following exon of the β1 integrin gene (KI^{lox}; Fig. 2, A and B).

To exclude adverse effects of the intronic loxP sites, we established mice carrying only a loxP site in front of exon 15 or 16 but no mutation in the exons ($E15^{lox}$ and $E16^{lox}$). Homozygous $E15^{lox/lox}$ and $E16^{lox/lox}$ animals were born at the expected Mendelian ratio, were fertile, had a normal life span, and did not display any overt phenotype (Fig. S1, A and B, available at http://www.jcb.org/cgi/content/full/jcb.200604060/DC1; and not depicted). FACS analysis revealed normal expression and activation of β1 integrin (Fig. S4).

Because impaired β1 integrin function severely affects interfollicular epidermis and hair follicle cycling (Brakebusch et al., 2000), we chose to more closely investigate the skin of these mice for defects. $E15^{lox/lox}$ and $E16^{lox/lox}$ showed normal skin development, and no hyperthickening of the epidermis, blister formation, or dermal fibrosis could be observed. Similarly, the hair follicle frequency, length, and morphology were unaffected in $E15^{lox/lox}$ and $E16^{lox/lox}$ mice (Fig. S1, C and D).

Finally, RT-PCR analysis of the cytoplasmic domain of the β1 integrin mRNA from lox/lox wild-type and lox/lox mutant keratinocytes revealed a normal level of β1 integrin expression and faithful splicing of the cytoplasmic exons to generate the β1A mRNA (Fig. 2 G). RNA samples from striated muscle were used to amplify the muscle-specific exon D β1 integrin isoform (β1D). Neither the introduction of the loxP site upstream of exon 15 or 16 nor the point mutations in exon 15 or exon 16 led to isoform switching. Altogether, these findings indicate that the presence of the single loxP in the intron preceding exon 15 or 16 of the β1 integrin gene did not affect integrin expression and function.

D759A mutation does not affect β1 integrin function

Homozygous D/A mutant mice lacking the salt bridge connecting the β1 and α subunits were born at the Mendelian ratio

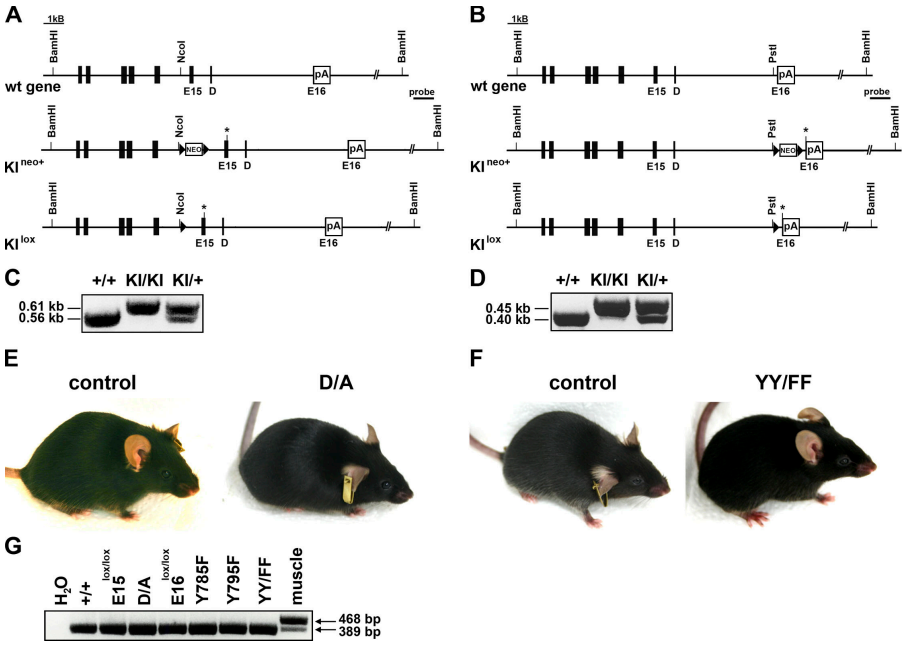

Figure 2. **Targeting strategy for introducing point mutations in the cytoplasmic domain of the β1A integrin.** (A and B) Partial map of the β1A wild type (wt), the KI allele with a point mutation (indicated by asterisk) in exon 15 (E15; A) or exon 16 (E16; B), respectively, before (KI^{neo+}) and after (KI^{lox}) Cre-mediated deletion of the floxed neo cassette. The DNA fragment sizes obtained after BamHI restriction digest, as well as the probe used for Southern blotting are indicated. Filled boxes indicated exons, and triangles indicate loxP sites. D, exon D; neo, neomycin resistance gene; pA, polyadenylation signal. (C and D) Representative PCR genotyping of KI^{lox} mice using primers hybridizing to exons 14 and 16 of the β1 integrin cDNA from template RNA derived from keratinocytes of exon 15 and 16 control mice and KI littermates. The RNA samples from both the control and the mutant keratinocytes revealed a single PCR product of the expected size of 389 bp. The 468-kb band represents the transcript size for the wild-type β1D integrin mRNA, which is the muscle-specific isoform of the β1 integrin gene and only detectable in muscle RNA.

(not depicted), as determined by genotyping of the heterozygous D/A intercrosses (Fig. 2 C). The mutant mice were fertile and had a normal life span. Furthermore, D/A mutant mice had normal growth rates (Fig. S2, A and B, available at http://www.jcb.org/cgi/content/full/jcb.200604060/DC1) and did not display any obvious impairments (Fig. 2 E).

Detailed histological analysis of the mutant skin at postnatal day (P) 1, P7, P14, P21, and 3 mo revealed normal interfollicular epidermis, normal epidermal–dermal junction, and normal hair follicle formation and progression through the hair cycle (Fig. 3 A and not depicted). As in control skin, immunostaining of the D/A mutant skin showed β1 integrin and α6 integrin restricted to basal keratinocytes and laminin 5 (LN5) deposition at the dermal–epidermal junction (Fig. 3, B and C; and not depicted). Furthermore, proliferation as determined by BrdU incorporation was normal in the basal keratinocytes expressing the D/A mutant integrin, with 11.1 ± 0.07% BrdU-positive cells in control and 11.2 ± 2.26% in the D/A mutant mice in 14-d-old mice and 3.5 ± 0.14 and 3.7 ± 0.42% in 3-mo-old mice, respectively. Similarly, the proliferation of hair bulb cells was unaltered (unpublished data).

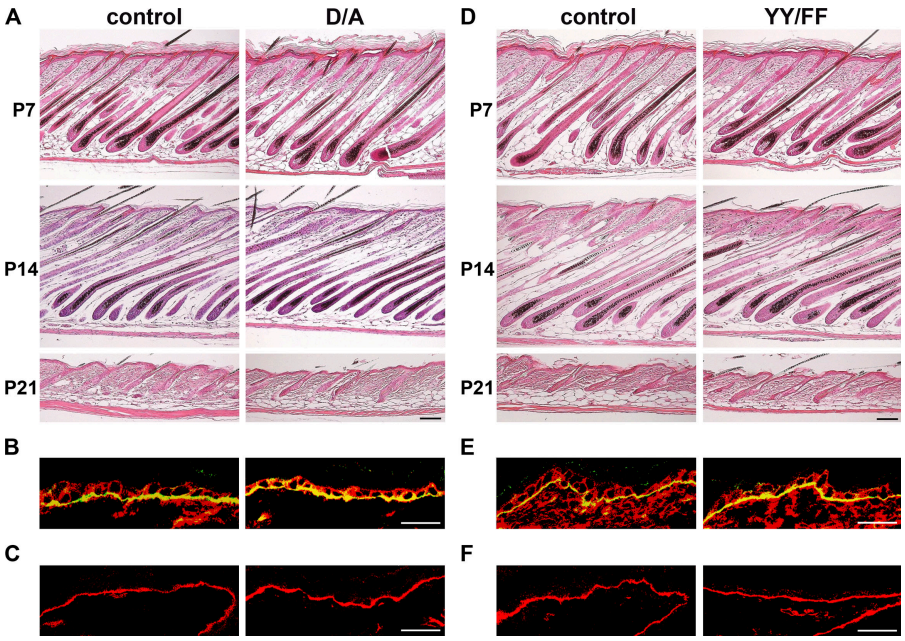

Figure 3. **Normal skin development in D/A and YY/FF mutant mice.** (A and D) HE-stained back skin of P7, -14, and -21 mice shows normal hair cycle progression in D/A (A) and YY/FF (D) mutant mice. (B and E) Back skin of 2-wk-old control and D/A (B) and YY/FF (E) mutant animals stained for β1 integrin (red) and α6 integrin (green). Immunostaining for β1 and α6 integrin subunits reveals normal integrin expression in the skin. (C and F) Immunostaining of 2-wk-old back skin for LN5 shows normal LN5 deposition at the epidermal–dermal junction in control and mutant skin. Bars, 50 μm.

Tyrosine phosphorylation of the NPXY motifs is not required for development

To investigate the role of tyrosine phosphorylation of the β1 subunit for embryonic and postnatal development, we intercrossed heterozygous Y783F and Y795F mice, respectively. Surprisingly, both mutant mouse strains were viable and fertile (Fig. S1 E). The lack of an obvious phenotype in the single-tyrosine mutant mice prompted us to investigate mice in which both tyrosine residues were changed to phenylalanine (YY/FF). Astonishingly, the homozygous YY/FF mutant mice (Fig. 2 D) were also viable and fertile and, moreover, did not show any obvious phenotype. Their weight and size was comparable to the age-matched littermate controls at all time points analyzed (Fig. S2, C and D). Furthermore, histological analysis of back skin at P1, P7, P14, P21, and 6 mo did not reveal any abnormalities with respect to the morphology of the interfollicular epidermis and the hair follicles (Fig. 3 D and not depicted). Regardless of their age, YY/FF mutant mice displayed neither skin blisters nor signs of dermal fibrosis. Immunostaining of skin sections from 14-d- and 6-mo-old homozygous YY/FF mutant mice revealed normal expression of the β1 and α6 integrin subunits (Fig. 3 E and not depicted) and normal deposition and assembly of LN5 at the epidermal–dermal junction (Fig. 3 F and not depicted). Finally, the number of proliferating cells in the basal layer of the epidermis was not changed in the mutant skin, with 8.4 ± 0.14% BrdU-positive cells in control and 10 ± 0.21% in YY/YY mutant mice at 14 d of age and 3.55 ± 0.63 and 2.85 ± 0.78%, respectively, at 6 mo of age. Furthermore, the proliferation of hair bulb cells was similar in control and YY/FF mutant hair follicles (unpublished data).

Primary D/A and YY/FF mutant keratinocytes have normal adhesion, spreading, and migration in vitro

If loss of the salt bridge and prevention of tyrosine phosphorylation increase integrin activation, this should have consequences for β1 integrin–mediated adhesion, spreading, and migration. Although defects in these parameters were not obvious in the context of skin, we isolated primary keratinocytes to test these parameters in cellular assays.

Both the D/A and YY/FF mutant cells attached to a mixture of collagen I (Col1) and FN-coated surface, spread, and grew in a manner indistinguishable from control cells (unpublished data). In vitro–expanded D/A and YY/FF keratinocytes were assayed for their ability to adhere to increasing concentrations of LN5, Col1, and FN. Dose-dependent adhesion of D/A mutant keratinocytes (Fig. 4 A) and YY/FF mutant keratinocytes (Fig. 4 B) was comparable to their respective control cells on all matrix substrates analyzed (Fig. 4, A and B). Similarly, the D/A as well as the YY/FF mutant keratinocytes spread to a similar extent on a Col1/FN mixture as control cells (Fig. 4 C and not depicted).

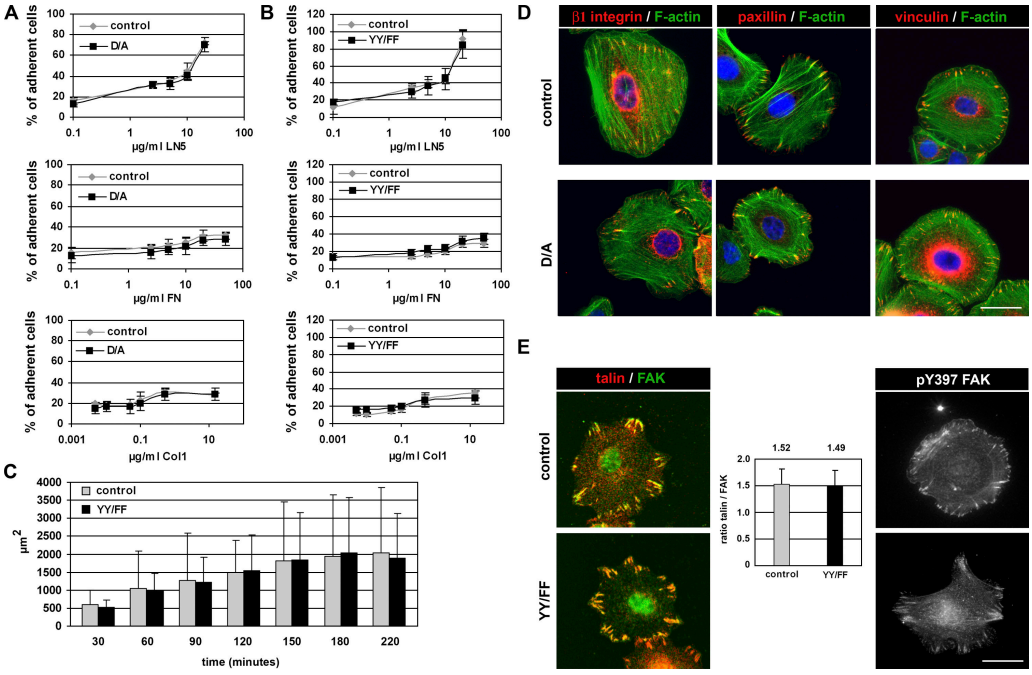

Figure 4. **D/A and YY/FF mutant keratinocytes adhere and migrate normally in vitro.** (A and B) Dose-dependent cell adhesion of D/A (A) and YY/FF (B) keratinocytes on LN5, FN, and Col1 is similar compared with control cells. Error bars indicate SD. Shown is the mean value of three independent experiments. (C) Control and YY/FF mutant keratinocytes were plated on Col1/FN-coated plastic and monitored by live cell imaging. Quantification of the cell area of 50 randomly selected cells per time point and genotype is shown. Error bars indicate SD. The extent of spreading of YY/FF mutant keratinocytes is not significantly different from control cells. (D) Keratinocytes were cultured for 2 d on a mixture of Col1 and FN and immunostained for β1 integrin, paxillin and vinculin (red), and F-actin (phalloidin; green). Nuclei were stained with DAPI (blue). Size and number of FAs and actin stress fibers is normal in D/A mutant keratinocytes. (E) Normal and YY/FF mutant keratinocytes were stained for talin (red), FAK (green), and pY397FAK upon plating on a mixture of Col1 and FN. Size and number of FAs and localization of talin, FAK, and pY397FAK is normal in YY/FF mutant keratinocytes. Bars shows ratiometric analysis of talin and FAK signals in talin/FAK double-immunostained YY/FF mutant keratinocytes. Shown is the mean value of 27 cells analyzed per genotype. The ratio of talin/FAK signals is identical in the FAs of the YY/FF mutant cells. Bars, 10 µm.

To investigate focal contact organization and F-actin distribution in mutant keratinocytes, cells were cultured for 2 d on a Col1/FN mixture and subsequently stained with antibodies against β1 integrin, talin, FAK, pY397FAK, vinculin and paxillin, and fluorescently labeled phalloidin. No obvious differences were observed in the size or number of focal adhesions (FAs) and in F-actin organization (Fig. 4, D and E; and Fig. S3, available at http://www.jcb.org/cgi/content/full/jcb.200604060/DC1). Similarly, the β1 integrin carrying either the D/A or YY/FF mutation localized normally to FAs (Fig. 4 D and Fig. S3). Furthermore, total FAK, pY397FAK, and talin were found in FAs of D/A and YY/FF mutant keratinocytes (Fig. 4 E and not depicted). To quantitatively assess the extent of talin recruitment into FA of the YY/FF mutant keratinocytes, we simultaneously stained mutant keratinocytes with anti-talin and anti-FAK antibodies and subsequently determined the ratio of the mean fluorescence intensities. The talin/FAK ratios were almost identical in FAs of control and YY/FF mutant cells (Fig. 4 E), suggesting that the YY/FF mutation does not result in increased talin recruitment to integrin adhesion sites.

To test migration of mutant keratinocytes in vitro, we performed transwell migration and scratch assays. In transwell assays, control or D/A or YY/FF mutant keratinocytes were plated in transwell motility chambers and allowed to migrate toward medium lacking or containing EGF. In neither the absence nor the presence of EGF was the extent of migration significantly different between control and D/A or control and YY/FF mutant keratinocytes (Fig. 5, A and B). In scratch assays, we wounded a keratinocyte monolayer and monitored wound closure over a period of 6 h. The results demonstrate that the YY/FF mutant keratinocytes closed the wound with a speed that was not significantly different from control cells (Fig. 5, C and D).

Hyperactivation of β1 integrin could lead to increased activation of downstream signaling molecules such as FAK or extracellular signal–regulated kinase (Erk). To assess the activation status of these integrin effectors, we analyzed wounding-induced phosphorylation of FAK and Erk in YY/FF keratinocytes. No significant difference was found between control and mutant cells either before or after wounding, suggesting that NPXY tyrosine phosphorylation is not crucial for inducing the activity of these effector molecules (Fig. 5 E).

No detectable alteration in the activation of β1 integrin in D/A and YY/FF mutant mice

Previous studies have suggested that both D/A and YY/FF mutations will result in constitutive activation of β1 integrin (Sakai et al., 1998a, 1998b). Because the results of our cellular assays were inconsistent with constitutively active β1 integrin, we examined integrin activation more closely on different primary cells by measuring the binding of the 9EG7 antibody, which recognizes an epitope that is exposed only on activated β1 integrins.

Freshly isolated keratinocytes from adult D/A mutant mice expressed β1, α2, α6, and β4 integrins at similar levels as control keratinocytes (Fig. 6 A). Recognition of the 9EG7 epitope of the β1 integrin identified a similarly small fraction of activated β1 integrins on D/A homozygous mutant and control keratinocytes (Fig. 6 A). Primary keratinocytes of YY/FF mutant mice had a slightly reduced expression of β1 integrin with a similar reduction of the 9EG7 epitope. Expression levels of α2 integrin were also slightly decreased, whereas α6 and β4 integrin were unchanged compared with control cells (Fig. 6 B).

The 9EG7 epitope is not easily detected on epidermal keratinocytes (Bazzoni and Hemler, 1998). In addition, the trypsin treatment during the preparation of the keratinocytes may abrogate the 9EG7 epitope. Therefore, we also analyzed the β1 integrin activation by FACS on granulocytes, macrophages, B-lymphocytes, and erythroblasts freshly isolated from the bone marrow of control and mutant mice (Fig. S4). Expression of β1 integrin was comparable between control and mutant cells, with the exception of the granulocytes and macrophages in YY/FF mice, which showed a reduction of surface β1 integrin by ∼50 and 30%, respectively (Fig. S4). We could not detect increased basal 9EG7 exposure on D/A and YY/FF mutant cells (Fig. S4). Interestingly, treatment of cells with 5 mM Mn^{2+} markedly increased the 9EG7 epitope

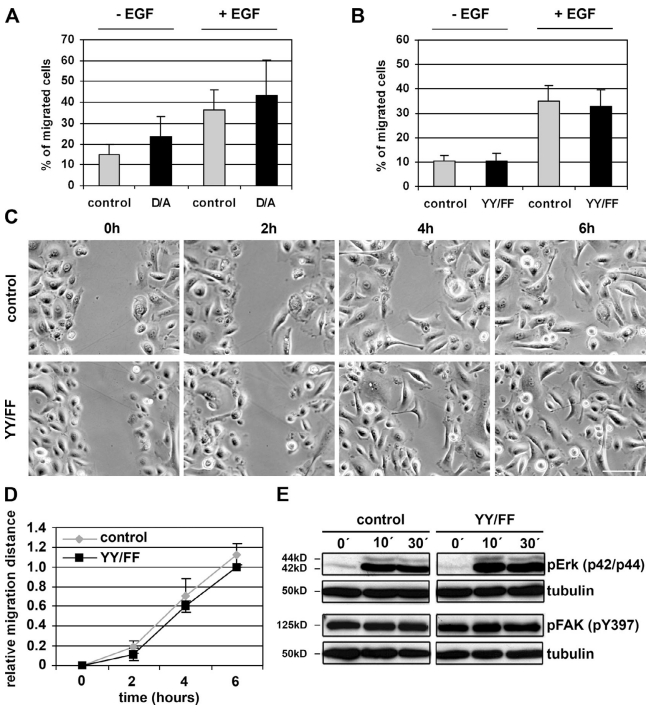

Figure 5. **Normal migration of the D/A and YY/FF keratinocytes in vitro.** (A and B) Migration of control, D/A mutant (A), and YY/FF (B) keratinocytes through transwell chambers. The bottom chamber contained medium with or without EGF, and cells from five randomly chosen fields that migrated to the bottom of the membranes were counted. Bars represent the number of migrated cells from three independent experiments. Error bars indicate SD. D/A and YY/FF mutant keratinocytes showed migration behavior similar to control cells. (C) Control and YY/FF keratinocytes were grown to confluence, and the cell monolayer was wounded using a blunted tip of a glass capillary. Pictures from the same area of the scratch were taken at the indicated time points. Data shown are from one experiment, which was repeated twice. Bar, 50 μm. (D) Migration was calculated by measuring the remaining width of the scratch. For each experiment, at least 10 areas were measured per time point. Error bars indicate SD. (E) Basal activity and wound-induced activation of pErk and pFAK does not significantly differ between starved (keratinocyte growth medium without FCS) control and YY/FF mutant keratinocytes. Tubulin served as a loading control.

exposure to a similar extent on control ($E15^{lox/lox}$ and $E16^{lox/lox}$) and D/A or YY/FF mutant cells (Fig. S4).

The assessment of ligand binding is an alternative method for evaluating integrin activation. To this end, we expressed and fluorescently labeled the central cell binding domain of FN (FNIII7-10), which is bound by the α5β1 integrin expressed on cultured primary keratinocytes. In the presence of 5 mM Mn^{2+} control, D/A (Fig. 6 C) and YY/FF (Fig. 6 D) mutant keratinocytes bound the Alexa 647–labeled FNIII7-10 in a dose-dependent manner and to a comparable extent (Fig. 6, C and D). As expected, the exposure to 2 mM EDTA or Tris-buffered saline alone revealed only very weak or no ligand binding on all cell types analyzed (Fig. 6, C and D).

β1 integrin carrying the YY/AA mutation is not functional in keratinocytes in vivo

Although heterozygous YY/AA mice were normal, homozygous YY/AA mutant mice died during embryonic development (unpublished data). To generate mice that express the YY/AA mutation only in keratinocytes, we intercrossed heterozygous YY/AA mutant animals with floxed β1 integrin mice expressing the Cre recombinase under the keratin 5 (K5) promoter (Brakebusch et al., 2000) to obtain β1(YY/AA/fl) K5-Cre (YY/AA) mice. Upon Cre-mediated deletion of the floxed β1 allele, only the YY/AA mutant allele is expressed in keratinocytes. The YY/AA mice were born without obvious abnormalities, but by 2 wk, skin pigmentation and hair coat development was markedly impaired (Fig. 7 A). At 5 wk of age, almost the entire hair coat was lost and wounds appeared in mechanically stressed regions (unpublished data). This phenotype closely resembled the abnormalities observed in mice with a keratinocyte-specific deletion of the β1 integrin gene (Brakebusch et al., 2000).

Histological analysis of skin sections further corroborated the similarities between the YY/AA and the β1 integrin–null mutation. The skin of 14-d-old YY/AA mutant mice displayed hyperthickened epidermis with aberrantly shaped cells, blister formation at the epidermal–dermal junction, and severe hair follicle abnormalities (Fig. 7, B and C).

To confirm that only the YY/AA-mutated β1 integrin was expressed in skin, we performed LacZ staining, the expression of which indicates the deletion of the floxed β1 integrin allele (Brakebusch et al., 2000). The LacZ staining was clearly detectable in the interfollicular epidermis and the outer root sheath of hair follicles derived from YY/AA mutant mice (Fig. 7 D). Immunostaining revealed that basal and suprabasal keratinocytes of mutant mice express β1 integrin (Fig. 7 E, arrowheads indicate suprabasal expression), although the staining was partially discontinuous (not depicted). Similarly, the staining of the α6 integrin was discontinuous. Interestingly, β1 integrin is expressed in regions of skin blistering, suggesting that the mutant

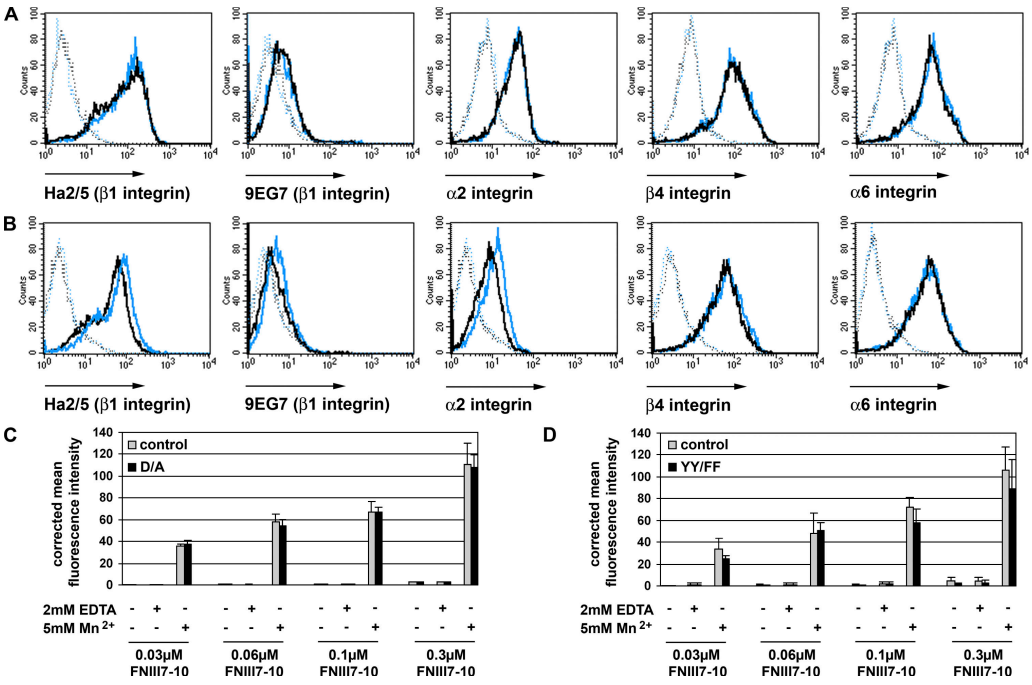

Figure 6. **Integrin expression and activation on D/A and YY/FF mutant keratinocytes.** (A and B) Cell surface expression of integrins in freshly isolated keratinocytes from adult mice assessed by FACS analysis. Keratinocytes are stained with antibodies against β1, α2, β4, and α6 integrins and the 9EG7 epitope of β1 integrins. (A) Blue and black histograms denote control and D/A mutant keratinocytes, respectively. The background fluorescence is shown as a dotted line. Mutant D/A keratinocytes show normal integrin expression and normal β1 activation. Shown are representative histograms from three independent experiments. (B) Blue and black histograms denote control and YY/FF mutant keratinocytes, respectively. The expression level of β1 and α2 integrins is reduced on YY/FF keratinocytes when compared with the keratinocytes from control mice. The levels of β4 and α6 integrins are normal. Staining with the 9EG7 antibody reveals reduced signals on the YY/FF keratinocytes corresponding to the reduced expression of the β1 integrin subunit. Shown are representative histograms from three independent experiments. (C and D) Ligand binding properties of cultured primary keratinocytes. Cells were incubated with increasing concentrations of Alexa 647–labeled FNIII7-10 fragment in the absence (−) or presence (+) of 2 mM EDTA or 5 mM $MnCl_2$, respectively, and analyzed by FACS. FNIII7-10 binding was similar between the mutant D/A (C) or YY/FF (D) keratinocytes and their respective controls. Mean fluorescence intensities were corrected for background fluorescence values. Error bars indicate SD. Shown is the mean of three independent experiments.

integrin is nonfunctional (Fig. 7 E, arrows). In 14-d-old mutant mice, LN5 was diffusely deposited at the epidermal–dermal junction in a manner similar to the β1-deficient epidermis (Fig. 7 F).

To quantitatively assess the integrin levels on keratinocytes, we performed FACS analysis with freshly isolated keratinocytes from 6-d-old control and YY/AA mutant mice. The levels of β1, β4, and α6 integrin were reduced by ∼50% and the levels of α2 integrin by ∼25% (Fig. 8 A). 9EG7 staining revealed almost no signal on YY/AA keratinocytes, in contrast to controls, suggesting that YY/AA integrins are present in an inactive conformation on mutant keratinocytes (Fig. 8 A).

The YY/AA mutant keratinocytes do not display the 9EG7 epitope and show a 50% reduction of the β1 integrin expression on the cell surface. To confirm that the skin phenotypes in mutant mice arose from the loss of talin–β1 integrin tail interaction and defective integrin activation and not from the reduced integrin expression, we established a mouse strain carrying a hypomorphic, wild-type β1 integrin allele (*hpm*). The *hpm* mouse strain was obtained by fusing a 141-bp cDNA fragment encoding the cytoplasmic domain of the β1 integrin gene in frame into exon 15, just behind the transmembrane span encoding sequence (Fig. S5, available at http://www.jcb.org/cgi/content/full/jcb.200604060/DC1). Homozygous mice carrying the *hpm* allele died during development (unpublished data). To express the *hpm* mutation exclusively in keratinocytes, we intercrossed *hpm* mice with floxed β1 integrin mice expressing the Cre recombinase under the K5 promoter (Brakebusch et al., 2000). Although freshly isolated *hpm* keratinocytes expressed only ∼25% of the normal β1 integrin level on their surface (Fig. 8 B), they developed a milder phenotype when compared with the YY/AA, which express 50% of the mutant β1 integrin (Fig. 7 A). At 2 wk of age, the hair coat of the *hpm* mice was slightly reduced and only a few of the *hpm* hair follicles were misshapen and resembled the YY/AA or K5-β1 phenotype (Fig. 7 B). Similarly, the degree of epidermal hyperthickening, aberrant shape of basal keratinocytes, and extent of blistering was much less prominent in the *hpm* mice when compared with the YY/AA or K5-β1 mutant mice (Fig. 7 C and not depicted). LN5 deposition at the dermal–epidermal junction was broadened in *hpm* skin, although to a much lesser extent when compared with YY/AA and K5-β1 mutant skin (Fig. 7 F). Altogether, these data suggest that the phenotypic alterations observed in YY/AA mutant mice are likely caused by an impairment of the talin–β1 integrin tail interaction, rather than a reduced β1 integrin expression.

YY/AA keratinocytes show impaired adhesion and an aberrant cytoskeleton in vitro

To analyze adhesion and cytoskeleton of YY/AA keratinocytes, freshly isolated mutant keratinocytes were seeded on

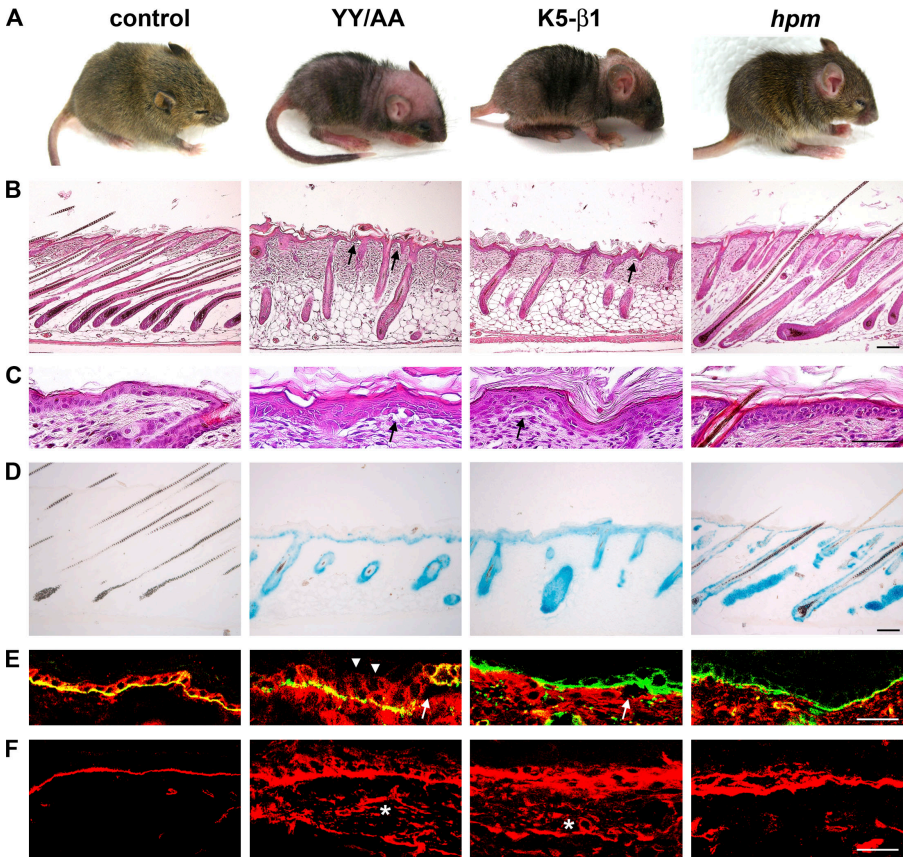

Figure 7. **Keratinocyte-restricted expression of the YY/AA mutation in the β1A integrin cytoplasmic domain.** (A) Control, YY/AA mutant, K5-β1 mutant, and *hpm* mutant mice at the age of 2 wk. YY/AA mutant and K5-β1 mutant mice have a reddish skin with a reduced number of hairs and blisters, whereas the hair coat of the *hpm* mice is only mildly affected. (B) HE-stained paraffin sections of back skin derived from P14 mice show aberrant hair follicle morphogenesis of the skin. The mutant hair follicles fail to grow as deeply into the subcutis as in the littermate control mice and are abnormally shaped. YY/AA and K5-β1 mutant mice have a hyperthickened epidermis and blisters between the epidermis and dermis (arrows). The *hpm* skin displays an intermediate phenotype. (C) High magnification of the HE-stained back skin section showing blister formation (arrows) and aberrant morphology of the basal keratinocytes in YY/AA and K5-β1 mutant mice. (D) Control, YY/AA mutant, K5-β1 mutant, and *hpm* mutant epidermis examined for LacZ activity as a readout of Cre-mediated β1 integrin gene deletion. LacZ-positive cells are visible in the epidermis and hair follicles of the YY/AA, K5-β1, and *hpm* mutant mice. (E) Immunostaining of β1 (red) and α6 (green) integrins. Both integrin subunits are expressed on the surface of basal and suprabasal keratinocytes (arrowheads) in the back skin section from P14 YY/AA mutant mice. Blistering occurs independently of the β1 integrin expression (arrows), suggesting a nonfunctional integrin. β1 integrin expression is not detectable in K5-β1 and *hpm* mutant mice. Integrin α6 expression is discontinuous in YY/AA and K5-β1 mutant mice and normal in the *hpm* mice. (F) Similar to the conditional deletion of the β1 integrin gene in skin, introduction of the YY/AA mutation leads to diffuse LN5 deposition in the dermis of the mutant mice (asterisks). Basement membrane organization is only partially affected in the *hpm* mice. Bars, 50 μm.

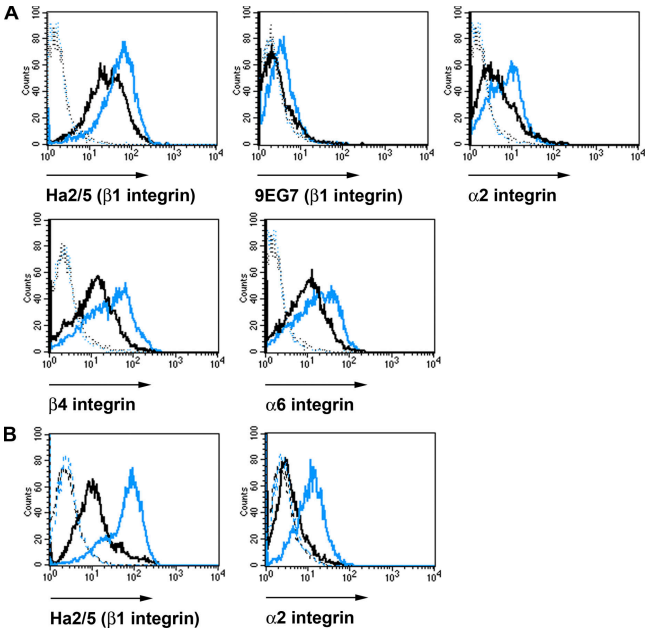

Figure 8. **Reduced integrin expression and activation on YY/AA mutant keratinocytes.** Cell surface expression of integrins on freshly isolated keratinocytes from 6-d-old YY/AA (A) and 2.5-mo-old *hpm* mice (B) analyzed by FACS. (A) YY/AA keratinocytes are stained with antibodies against β1, α2, β4, and α6 integrins and the 9EG7 epitope of β1 integrins. Blue and black histograms denote control and YY/AA mutant keratinocytes, respectively. Mutant YY/AA keratinocytes display a strongly reduced expression of β1, α2, β4, and α6 integrins and an almost complete absence of 9EG7 signals. (B) *hpm* keratinocytes are stained with antibodies against β1 and α2 integrins. Blue and black histograms denote control and *hpm* mutant keratinocytes, respectively. Fusion of a wild-type 141-bp cDNA fragment encoding the cytoplasmic domain of the β1 integrin gene in frame into exon 15 of the β1 integrin gene reduces β1 integrin cell surface expression to 25% of wild-type expression levels. The background fluorescence is shown as a dotted line. Shown are representative histograms from three independent experiments.

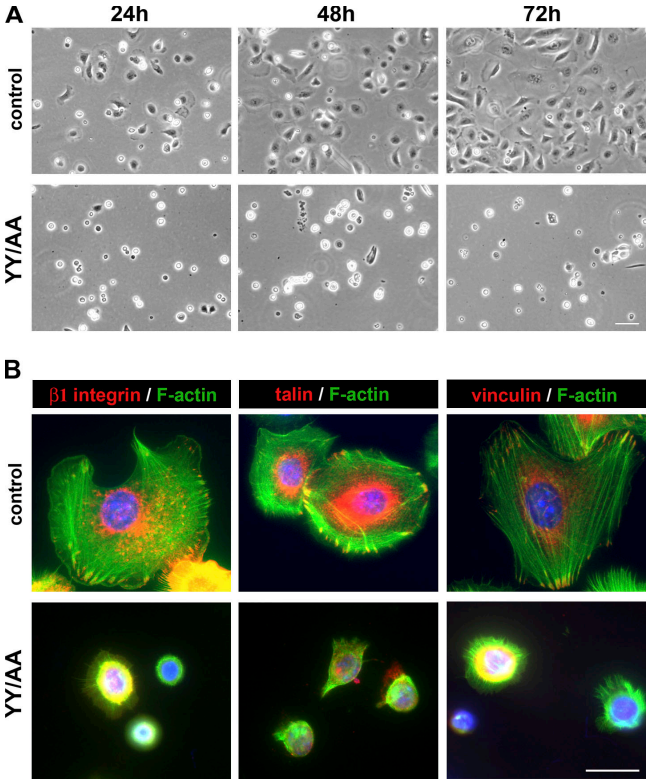

Figure 9. **Defective adhesion and spreading of YY/AA primary keratinocytes.** (A) Freshly isolated keratinocytes plated at the same density on a mixture of Col1 and FN. Although control cells are well spread, mutant cells do not spread and adhere properly. Cells at the indicated time points after seeding are shown. Bar, 25 μm. (B) Keratinocytes were cultured for 2 d on a mixture of Col1 and FN and immunostained for β1 integrin, talin, vinculin (red), and F-actin (phalloidin; green). Nuclei were stained with DAPI (blue). YY/AA mutant cells fail to develop FAs and to organize the actin cytoskeleton. Shown are representative pictures from three independent experiments. Bar, 10 μm.

Col1/FN-coated plastic dishes. The majority of control cells appeared well spread 24 h after plating and were confluent 72 h later. In sharp contrast, only a few mutant cells were attached 24 h after seeding. They appeared round and failed to spread and proliferate (Fig. 9 A).

Immunostaining of the few adherent cells (cultured for 2 d on Col1 and FN) for β1 integrin, paxillin, and vinculin revealed a complete absence of FAs and stress fibers and the formation of F-actin clumps and/or fine F-actin filaments extending radially from the perinuclear region to the plasma membrane. Almost the entire immune signal of β1 integrins and the FA components was found within the cytoplasm (Fig. 9 B). Altogether, these data suggest that the YY/AA mutation in the cytoplasmic domain of β1 integrins renders the integrins inactive.

Discussion

A key feature of integrins is their ability to switch between an inactive and an active conformation. It is believed that talin binding to the cytoplasmic domain of the β subunit disrupts the α/β tail interaction, leading to tail separation and changes in the conformation of the extracellular domain, consistent with integrin activation (Humphries et al., 2003; Calderwood, 2004). In the present study, we report the phenotypic analysis of mouse strains, which harbor point mutations in either the talin binding motif or the membrane-proximal salt bridge of the β1 integrin subunit.

It has been shown that the substitution of the tyrosine residue with alanine in the proximal NPXY motif of β tails is sufficient to inhibit binding of talin and lock integrins in an inactive conformation (Tadokoro et al., 2003). To examine the consequences of this finding during the development of a multicellular organism, we generated mice in which we substituted the tyrosine residues in the proximal and distal NPXY motifs of the β1 integrin subunit with alanine. We obtained compelling evidence that functional NPXY motifs are required for β1 integrin function both in vivo and in vitro. First, mice with a homozygous YY783/795AA (YY/AA) mutation die during development. Second, expression of the YY/AA mutation specifically in keratinocytes mirrored the β1 integrin–null skin phenotype (Brakebusch et al., 2000) with epidermal hyperplasia, skin blistering, abnormal distribution of basement membrane proteins, and a dermal fibrosis. Finally, primary keratinocytes from YY/AA mutant skin did not express detectable activated (9EG7-positive) β1 integrins and exhibited severely

compromised integrin functions characterized by profound adhesion defects, impaired spreading, FA assembly, and F-actin distribution. The YY/AA mutant keratinocytes expressed only ~50% of the normal β1 integrin level on their cell surface. Reduced surface expression of β1 integrin in the absence of talin binding is in agreement with a previous report showing that talin controls β1 integrin exit from an early compartment of the secretory pathway (Martel et al., 2000). To exclude the possibility that the reduced integrin levels rather than the abolished integrin activation is responsible for the YY/AA phenotype, we generated a hypomorphic β1 integrin mouse strain expressing only ~25% of wild-type β1 integrins on keratinocytes. The hypomorphic mouse strain developed a much milder skin phenotype than the defects observed in the YY/AA mutant mice, which clearly suggests that loss of integrin activation rather than the reduced expression is responsible for the severe skin and hair abnormalities in YY/AA mutants.

Because integrins can quickly switch between an active and an inactive conformation, the binding of talin to the β integrin tails must be tightly and efficiently regulated. Several studies reached the conclusion that this regulation may be achieved by reversibly phosphorylating the tyrosine residues of the β tail. In this model, tyrosine phosphorylation of the β tail NPXY motif by Src family kinases inhibits talin binding and displaces β1 integrins from FA sites (Johansson et al., 1994; Sakai et al., 2001; Datta et al., 2002). Inhibiting phosphorylation of the NPXY motif by substituting the tyrosine with a nonphosphorylatable phenylalanine resulted in enhanced FN binding and assembly (Sakai et al., 1998a), which was suggested to be due to enhanced talin binding to the NPXF motif.

We tested the role of tyrosine-783 and -795 phosphorylation in vivo by substituting either each tyrosine individually (Y783F and Y795F) or both together (YY783/795FF; YY/FF) with phenylalanine. Surprisingly, the mice with a single tyrosine mutation displayed no obvious defects. Moreover, mice with mutations in both tyrosine residues were also born without phenotypic changes. When we searched the skin of YY/FF for subtle defects, we found normal keratinocyte layers in the epidermis, normal keratinocyte proliferation, regular distribution of basement membrane proteins, absence of skin blisters, and normal hair follicle formation and cycling. Moreover, adhesion, spreading, FA formation and distribution, F-actin organization, and migration were unaffected in freshly isolated YY/FF mutant keratinocytes.

The absence of abnormalities in YY/FF mice strongly indicates that the mutant β1 integrin cytoplasmic tail is still able to recruit talin and activate the integrin. Furthermore, the in vivo findings also indicate that the YY/FF mutation still allows switching β1 integrins between active and inactive conformations. Several additional experiments confirm this notion. First, we found the surface levels of β1 integrins detected with an activation-associated epitope increased neither on keratinocytes nor on hematopoietic cells. Second, we could induce integrin activation with Mn^{2+} on keratinocytes and different hematopoietic cells to a similar extent as on the corresponding control cells. Finally, migration-induced integrin activation triggered comparable FAK and Erk phosphorylation (outside-in signaling) in YY/FF mutant and control keratinocytes. These observations allow some important conclusions: first, β1 integrin cytoplasmic tyrosine phosphorylation is dispensable to reverse talin-mediated integrin activation under physiological conditions. It is possible that NPXF bound talin is released from the mutant β1 integrin cytoplasmic domain by other β1 tail binding proteins, such as integrin cytoplasmic domain–associated protein (ICAP-1; Bouvard et al., 2003) or filamin (Kiema et al., 2006). Second, β1 integrin cytoplasmic tyrosine phosphorylation plays no obvious role in integrin outside-in signaling, although an increasing number of proteins are capable of binding the NPXY motifs, including myosin X and Kindlin-1 (Kloeker et al., 2004; Zhang et al., 2004). However, it also possible that the integrin NPXY phosphorylation plays an important role during stress situations such as wound healing or inflammation, where cells move at high speed to restore tissue integrity. Such experiments are currently being performed in our laboratory.

The disruption of the membrane-proximal salt bridge between the α/β tails and their separation were suggested to be important steps toward integrin activation. Surprisingly, however, the destruction of this salt bridge by the substitution of the aspartic acid 759 with an alanine (D759A; D/A) in the β1 membrane-proximal region produced no obvious phenotype. Furthermore, freshly isolated keratinocytes or hematopoietic cells from the bone marrow of control and D/A mutant mice expressed low but similar levels of activated β1 integrins on their surface. Incubation of D/A mutant primary bone marrow cells with Mn^{2+} induced integrin activation (as assessed with the 9EG7 antibody) to an extent similar to corresponding control cells. Moreover, adhesion, spreading, and migration of D/A mutant keratinocytes through transwell chambers was unaffected by the disruption of the α/β1 integrin salt bridge. Together, these data indicate that the genetic disruption of the membrane-proximal salt bridge between the α and the β1 integrin subunits neither locks β1 integrins in a more activated state nor increases their sensitivity to activation-inducing agents such as Mn^{2+}, permitting normal integrin function in vivo and in vitro.

Although our findings indicate that the salt bridge between the α and the β cytoplasmic domain plays no rate-limiting role for development and postnatal life of mice, previous biochemical and cell biological studies have demonstrated that the salt bridge plays an important function in integrin activation (Hughes et al., 1996), integrin clustering (Cluzel et al., 2005), and cell migration (Sakai et al., 2001). Interestingly, structural analysis of the αIIβ and β3 tails by nuclear magnetic resonance spectroscopy also produced conflicting results. Although one group reported an interaction (Vinogradova et al., 2002, 2004), albeit a very weak one, two other reports failed to detect α/β tail interactions (Li et al., 2001; Ulmer et al., 2001). It is possible that the weak, handshake-like interaction between the α/β tail exists but plays a less important role as long as other α/β interactions are present, for example, in the membrane-spanning helical regions (Gottschalk et al., 2002; Schneider and Engelman, 2004). This can be rigorously tested by introducing specific mutations into the transmembrane domain of β integrin subunits.

Materials and methods

Generation of mutant mice

Mouse genomic clones used to generate the targeting constructs were described previously (Fässler and Meyer, 1995). The loxP-flanked neomycin cassette was inserted into either the NcoI site upstream of exon 15 (Fig. 2 A) or into the PstI site upstream of exon 16 (Fig. 2 B). Both constructs were used to produce mice ($E15^{neo+}$ and $E16^{neo+}$). Point mutations were introduced in exon 15 and 16 using the AlteredSites II in vitro mutagenesis system (Promega). The D/A mutation was subsequently transferred into the $E15^{neo+}$ construct, and the F and A mutants were introduced into the $E16^{neo+}$ construct. The targeting constructs were electroporated into R1 ES cells. ES cell clones that underwent homologous recombination were isolated, identified by Southern blot using BamHI-digested genomic DNA and a 1-kb 3′ external probe, and injected into blastocysts to generate germline chimeras. Upon germline transmission, mutant mice were intercrossed with deleter-Cre transgenic mice (Betz et al., 1996) to obtain heterozygous $E15^{lox}$, $E16^{lox}$, D/A, Y783F, Y795F, YY/FF, and YY/AA mutant mice, which were subsequently interbred to obtain homozygous mutant mice. For all experiments performed with these mouse lines, either heterozygous or wild-type littermates served as control animals. Because YY/AA mutants were embryonic lethal, they were intercrossed with mice carrying a floxed β1 integrin gene (Brakebusch et al., 2000) and mice carrying K5 promoter-driven Cre recombinase transgene (Ramirez et al., 2004). Littermates carrying the floxed and the YY/AA mutated β1 integrin allele without the Cre recombinase transgene served as controls for experiments performed with the YY/AA mutant. Genotyping was performed by Southern blot or PCR using DNA isolated from tail biopsies. All animal studies were approved by the Regierung von Oberbayern.

RT-PCR

For RT-PCR, 50 ng of total RNA were reverse-transcribed using the iScript synthesis kit (Bio-Rad Laboratories), according to the manufacturer's protocol. The single-strand cDNA was used as a template for a PCR reaction, using a forward primer hybridizing to exon 14 (5′-AGGACATTGATGACTG-CTGG-3′) and a reverse primer hybridizing to exon 16 (5′-CCAAAACTA-CCCTACTGTGAC-3′) of the β1 integrin gene.

Histology and immunofluorescence

Hematoxylin-eosin (HE) and immunofluorescence staining were performed as described previously (Brakebusch et al., 2000). Because freshly isolated keratinocytes adhere and spread slowly on ECM substrata, all immunostainings on primary cells were performed after 48 h. BrdU staining was performed according to the manufacturer's instructions (Roche Diagnostics). β-Galactosidase activity was determined as previously described (Fässler and Meyer, 1995).

The following antibodies were used: β1 integrin (Chemicon), LN5 (laminin-γ2 chain; provided by T. Sasaki, Max Planck Institute of Biochemistry, Martinsried, Germany), BrdU-POD (Roche Diagnostics), paxillin (BD Biosciences), α6 integrin–FITC (BD Biosciences), vinculin (Sigma-Aldrich), talin (Sigma-Aldrich), phalloidin–Alexa 488 (Invitrogen), FAK (Upstate Biotechnology), phospho(p)-Y397FAK (Biosource International), p42/p44 MAPK (Cell Signaling), and α-tubulin (clone YL1/2; provided by J. Wehland, German Research Center for Biotechnology, Braunschweig, Germany). Fluorescence-conjugated secondary antibodies (goat anti–rat-Cy3, goat anti–mouse Cy3, goat anti–rabbit FITC, and donkey anti–rabbit Cy3) were purchased from Jackson ImmunoResearch Laboratories, and goat anti–rabbit Alexa 488 was obtained from Sigma-Aldrich. Antibodies were diluted according to the recommendation of the manufacturer.

Images were collected by confocal microscopy (DMIRE2; Leica) using Leica Confocal Software version 2.5 Build 1227 with 40× or 63× oil objectives, by fluorescence microscopy (DMRA2; Leica) using SimplePCI software (version 5.1.0.0110; GTI Microsystems) with 63× oil objectives, or by bright field microscopy (Axiovert; Carl Zeiss MicroImaging, Inc.), using IM50 software (Leica) with 10× or 40× objectives. All images were collected at RT. Immunofluorescence staining intensities from talin and FAK confocal images (detected by Cy3- and Alexa 488–coupled secondary antibodies, respectively) were quantified using the Leica Confocal Software. In brief, confocal stacks with highest talin fluorescence intensities were selected, and single FAs were selected for quantification. The mean fluorescence amplitude of talin and FAK of each FA was used to perform the ratiometric analysis shown in Fig. 4 E. Images were processed with Photoshop (Adobe).

Isolation of primary keratinocytes, adhesion, spreading, and migration assays

Primary keratinocytes were isolated from P6 or adult mice according to Romero et al. (1999) and grown to confluence on a mixture of Col1 (Cohesion) and 10 μg/ml FN (Invitrogen) coated plastic in keratinocyte growth medium containing 8% chelated FCS (Invitrogen) and 45 μM Ca^{2+}.

To test keratinocyte migration, transwell chambers (Falcon) with 8-μm-diameter pores were coated on the lower surfaces with a mixture of Col1 and 10 μg/ml FN. In duplicate assays, 4×10^4 primary keratinocytes were suspended in 45 μM calcium-containing Eagle's minimum essential medium (Sigma-Aldrich) supplemented with 1× L-glutamine (Invitrogen) and seeded onto the transwell chambers. The chambers were placed in keratinocyte growth medium with or without 50 ng/ml EGF (Sigma-Aldrich) and incubated for 14 h at 37°C. Afterward, cells in the upper surface of the membrane were removed and the cells on the lower surface fixed and stained with 20% methanol/0.1% crystal violet. The relative number of migrated cells (compared with the number of all attached cells) was determined from five randomly chosen microscopic fields of ∼1.2 mm^2 per duplicate experiment.

Cell adhesion of primary keratinocytes to LN5 (provided by M. Aumailley, University of Cologne, Cologne, Germany), FN, and Col1 was assayed as described previously (Hamelers et al., 2005). All experiments have been performed in duplicate.

To assess the spreading kinetics of primary keratinocytes, cells were plated on mixture of Col1 and 10 μg/ml FN–coated plastic and monitored at 37°C in 5% CO_2 by phase-contrast live cell imaging microscopy using a microscope (Axiovert 200M ; Carl Zeiss MicroImaging, Inc.) coupled to a camera (Visitron Systems). Images were collected with 10× objective. The cell area of 50 randomly selected cells per time point and genotype was quantified using MetaMorph 6.0 software (Molecular Devices). Wound healing assays and the measurement of the activity of signaling molecules upon wounding was performed as described previously (Czuchra et al., 2005).

Expression of FN fragment FnIII7-10

An expression plasmid (obtained from H.P. Erickson, Duke University Medical Center, Durham, NC) encoding a His-tagged version of FN type III repeats 7–10 (FnIII7-10) containing the central cell binding domain (Ohashi and Erickson, 2005) was used to express FnIII7-10 in *Escherichia coli*. Recombinant FnIII7-10 polypeptides were purified by TALON Metal Affinity chromatography according to the manufacturer's instructions (BD Biosciences). The final preparation was dialyzed in PBS. To label FnIII7-10 polypeptides with a fluorescent probe, the purified fragment (2 mg/ml) was first adjusted to pH 8.4 and subsequently incubated with 1 mg of Alexa Fluor 647 carboxylic acid and succidimidyl ester (Invitrogen) for 1 h at RT. The uncoupled probe was removed by dialysis in two changes of PBS at 4°C.

FNIII7-10 binding assay

To assess ligand binding properties of primary keratinocytes, confluent cells were harvested and incubated (3×10^5 cells per sample) with Alexa 647–coupled FNIII7-10 fragment in Tris-buffered saline in the presence or absence of 2 mM EDTA or 5 mM $MnCl_2$ and, finally, subjected to flow cytometry analysis.

Flow cytometry

Freshly isolated keratinocytes (5×10^5 cells per sample) were stained with antibodies against α6 integrin, α2 integrin, β1 integrin (Ha2/5 epitope; recognizes all β1 integrin subunits), β1 integrin (9EG7 epitope; recognizes an activation-associated epitope and hence only activated β1 integrins), or β4 integrin and subjected to FACS analysis (Potocnik et al., 2000). All antibodies were either FITC labeled or unlabeled and used in a 1:200 dilution, except 9EG7, which was used in a 1:100 dilution. Unlabeled antibodies were visualized with FITC α-rat IgG_{2a} (1:200). All antibodies were obtained from BD Biosciences. Dead cells were excluded from FACS analysis by the addition of 2.5 μg/ml propidium iodide before FACS analysis (FACSCalibur CellQuest Pro Software; Becton Dickinson).

Freshly prepared single-cell bone marrow suspensions (10^6 cells per sample; Rutherford and Schook, 1992) were stained with the β1 integrin–specific antibodies Ha2/5 or 9EG7 in Tris-buffered saline, containing 3% BSA with or without 5 mM $MnCl_2$ (Bazzoni and Hemler, 1998). In addition, cells were counterstained with antibodies against CD45R/B220 (B cell marker), Ly6G/Gr-1 (granulocyte marker), CD11b/Mac-1 (macrophage marker), or Ly-76/Ter-119 (erythroblast/erythrocyte marker), which were either PE-labeled or biotinylated. Biotinylated antibodies were detected with Streptavidin-Cy5 (Jackson ImmunoResearch Laboratories).

Online supplemental material

Fig. S1 shows the development of the lox/lox mice and mice carrying a single Y/F mutation. Fig. S2 shows the weight and size of aging D/A and YY/FF mutant mice. Fig. S3 shows the FA and stress fiber formation in YY/FF mutant keratinocytes. Fig. S4 shows the β1 integrin expression and activation on $E15^{lox/lox}$, D/A, $E16^{lox/lox}$, and YY/FF bone marrow cells. Fig. S5 shows the targeting strategy used to obtain the *hpm* mice. Online supplemental material is available at http://www.jcb.org/cgi/content/full/jcb.200604060/DC1.

We thank the members of the Fässler Laboratory for many dedicated discussions, Carsten Grashoff and Siegfried Ussar for careful reading of the manuscript, Michal Grzejszczyk for expert technical assistance, and Dr. Harold P. Erickson for providing the FNIII7-10 expression vector.

K.R. Legate is a recipient of the Marie Curie International Fellowship within the Sixth European Community Framework Programme. We gratefully acknowledge support from the Bundesministerium für Bildung und Forschung, the European Community (QLG1-CT-2001-00863), and the Max Planck Society.

Submitted: 11 April 2006
Accepted: 8 August 2006

References

Adair, B.D., J.P. Xiong, C. Maddock, S.L. Goodman, M.A. Arnaout, and M. Yeager. 2005. Three-dimensional EM structure of the ectodomain of integrin αVβ3 in a complex with fibronectin. *J. Cell Biol.* 168:1109–1118.

Arnaout, M.A., B. Mahalingam, and J.P. Xiong. 2005. Integrin structure, allostery, and bidirectional signaling. *Annu. Rev. Cell Dev. Biol.* 21:381–410.

Bazzoni, G., and M.E. Hemler. 1998. Are changes in integrin affinity and conformation overemphasized? *Trends Biochem. Sci.* 23:30–34.

Bennett, J.S. 2005. Structure and function of the platelet integrin alpha(IIb)beta(3). *J. Clin. Invest.* 115:3363–3369.

Betz, U.A., C.A. Vosshenrich, K. Rajewsky, and W. Muller. 1996. Bypass of lethality with mosaic mice generated by Cre-loxP-mediated recombination. *Curr. Biol.* 6:1307–1316.

Bouvard, D., L. Vignoud, S. Dupe-Manet, N. Abed, H.N. Fournier, C. Vincent-Monegat, S.F. Retta, R. Fassler, and M.R. Block. 2003. Disruption of focal adhesions by integrin cytoplasmic domain-associated protein-1 alpha. *J. Biol. Chem.* 278:6567–6574.

Brakebusch, C., and R. Fässler. 2005. beta1 integrin function in vivo: adhesion, migration and more. *Cancer Metastasis Rev.* 24:403–411.

Brakebusch, C., R. Grose, F. Quondamatteo, A. Ramirez, J.L. Jorcano, A. Pirro, M. Svensson, R. Herken, T. Sasaki, R. Timpl, et al. 2000. Skin and hair follicle integrity is crucially dependent on beta 1 integrin expression on keratinocytes. *EMBO J.* 19:3990–4003.

Calderwood, D.A. 2004. Integrin activation. *J. Cell Sci.* 117:657–666.

Cluzel, C., F. Saltel, J. Lussi, F. Paulhe, B.A. Imhof, and B. Wehrle-Haller. 2005. The mechanisms and dynamics of αvβ3 integrin clustering in living cells. *J. Cell Biol.* 171:383–392.

Cowan, K.J., D.A. Law, and D.R. Phillips. 2000. Identification of shc as the primary protein binding to the tyrosine-phosphorylated beta 3 subunit of alpha IIbbeta 3 during outside-in integrin platelet signaling. *J. Biol. Chem.* 275:36423–36429.

Critchley, D.R. 2005. Genetic, biochemical and structural approaches to talin function. *Biochem. Soc. Trans.* 33:1308–1312.

Czuchra, A., X. Wu, H. Meyer, J. van Hengel, T. Schroeder, R. Geffers, K. Rottner, and C. Brakebusch. 2005. Cdc42 is not essential for filopodium formation, directed migration, cell polarization, and mitosis in fibroblastoid cells. *Mol. Biol. Cell.* 16:4473–4484.

Datta, A., F. Huber, and D. Boettiger. 2002. Phosphorylation of beta 3 integrin controls ligand binding strength. *J. Biol. Chem.* 277:3943–3949.

Fässler, R., and M. Meyer. 1995. Consequences of lack of beta 1 integrin gene expression in mice. *Genes Dev.* 9:1896–1908.

Ginsberg, M.H., A. Partridge, and S.J. Shattil. 2005. Integrin regulation. *Curr. Opin. Cell Biol.* 17:509–516.

Gottschalk, K.E., P.D. Adams, A.T. Brunger, and H. Kessler. 2002. Transmembrane signal transduction of the alpha(IIb)beta(3) integrin. *Protein Sci.* 11:1800–1812.

Hamelers, I.H., C. Olivo, A.E. Mertens, D.M. Pegtel, R.A. van der Kammen, A. Sonnenberg, and J.G. Collard. 2005. The Rac activator Tiam1 is required for α3β1-mediated laminin-5 deposition, cell spreading, and cell migration. *J. Cell Biol.* 171:871–881.

Hughes, P.E., F. Diaz-Gonzalez, L. Leong, C. Wu, J.A. McDonald, S.J. Shattil, and M.H. Ginsberg. 1996. Breaking the integrin hinge. A defined structural constraint regulates integrin signaling. *J. Biol. Chem.* 271:6571–6574.

Humphries, M.J., P.A. McEwan, S.J. Barton, P.A. Buckley, J. Bella, and A.P. Mould. 2003. Integrin structure: heady advances in ligand binding, but activation still makes the knees wobble. *Trends Biochem. Sci.* 28:313–320.

Johansson, M.W., E. Larsson, B. Luning, E.B. Pasquale, and E. Ruoslahti. 1994. Altered localization and cytoplasmic domain-binding properties of tyrosine-phosphorylated β1 integrin. *J. Cell Biol.* 126:1299–1309.

Kiema, T., Y. Lad, P. Jiang, C.L. Oxley, M. Baldassarre, K.L. Wegener, I.D. Campbell, J. Ylanne, and D.A. Calderwood. 2006. The molecular basis of filamin binding to integrins and competition with talin. *Mol. Cell.* 21:337–347.

Kloeker, S., M.B. Major, D.A. Calderwood, M.H. Ginsberg, D.A. Jones, and M.C. Beckerle. 2004. The Kindler syndrome protein is regulated by transforming growth factor-beta and involved in integrin-mediated adhesion. *J. Biol. Chem.* 279:6824–6833.

Li, R., C.R. Babu, J.D. Lear, A.J. Wand, J.S. Bennett, and W.F. DeGrado. 2001. Oligomerization of the integrin alpha(IIb)beta(3): roles of the transmembrane and cytoplasmic domains. *Proc. Natl. Acad. Sci. USA.* 98:12462–12467.

Liddington, R.C., and M.H. Ginsberg. 2002. Integrin activation takes shape. *J. Cell Biol.* 158:833–839.

Luo, B.H., T.A. Springer, and J. Takagi. 2004. A specific interface between integrin transmembrane helices and affinity for ligand. *PLoS Biol.* 2:e153.

Martel, V., L. Vignoud, S. Dupe, P. Frachet, M.R. Block, and C. Albiges-Rizo. 2000. Talin controls the exit of the integrin alpha 5 beta 1 from an early compartment of the secretory pathway. *J. Cell Sci.* 113:1951–1961.

Ohashi, T., and H.P. Erickson. 2005. Domain unfolding plays a role in superfibronectin formation. *J. Biol. Chem.* 280:39143–39151.

Potocnik, A.J., C. Brakebusch, and R. Fassler. 2000. Fetal and adult hematopoietic stem cells require beta1 integrin function for colonizing fetal liver, spleen, and bone marrow. *Immunity.* 12:653–663.

Ramirez, A., A. Page, A. Gandarillas, J. Zanet, S. Pibre, M. Vidal, L. Tusell, A. Genesca, D.A. Whitaker, D.W. Melton, and J.L. Jorcano. 2004. A keratin K5Cre transgenic line appropriate for tissue-specific or generalized Cre-mediated recombination. *Genesis.* 39:52–57.

Romero, M.R., J.M. Carroll, and F.M. Watt. 1999. Analysis of cultured keratinocytes from a transgenic mouse model of psoriasis: effects of suprabasal integrin expression on keratinocyte adhesion, proliferation and terminal differentiation. *Exp. Dermatol.* 8:53–67.

Rutherford, M.S., and L.B. Schook. 1992. Differential immunocompetence of macrophages derived using macrophage or granulocyte-macrophage colony-stimulating factor. *J. Leukoc. Biol.* 51:69–76.

Sackstein, R. 2005. The lymphocyte homing receptors: gatekeepers of the multistep paradigm. *Curr. Opin. Hematol.* 12:444–450.

Sakai, T., Q. Zhang, R. Fassler, and D.F. Mosher. 1998a. Modulation of β1A integrin functions by tyrosine residues in the β1 cytoplasmic domain. *J. Cell Biol.* 141:527–538.

Sakai, T., O. Peyruchaud, R. Fassler, and D.F. Mosher. 1998b. Restoration of beta1A integrins is required for lysophosphatidic acid-induced migration of beta1-null mouse fibroblastic cells. *J. Biol. Chem.* 273:19378–19382.

Sakai, T., R. Jove, R. Fassler, and D.F. Mosher. 2001. Role of the cytoplasmic tyrosines of beta 1A integrins in transformation by v-src. *Proc. Natl. Acad. Sci. USA.* 98:3808–3813.

Schneider, D., and D.M. Engelman. 2004. Involvement of transmembrane domain interactions in signal transduction by alpha/beta integrins. *J. Biol. Chem.* 279:9840–9846.

Tadokoro, S., S.J. Shattil, K. Eto, V. Tai, R.C. Liddington, J.M. de Pereda, M.H. Ginsberg, and D.A. Calderwood. 2003. Talin binding to integrin beta tails: a final common step in integrin activation. *Science.* 302:103–106.

Takagi, J., and T.A. Springer. 2002. Integrin activation and structural rearrangement. *Immunol. Rev.* 186:141–163.

Ulmer, T.S., B. Yaspan, M.H. Ginsberg, and I.D. Campbell. 2001. NMR analysis of structure and dynamics of the cytosolic tails of integrin alpha(IIb)beta(3) in aqueous solution. *Biochemistry.* 40:7498–7508.

Vinogradova, O., A. Velyvis, A. Velyviene, B. Hu, T. Haas, E. Plow, and J. Qin. 2002. A structural mechanism of integrin alpha(IIb)beta(3) "inside-out" activation as regulated by its cytoplasmic face. *Cell.* 110:587–597.

Vinogradova, O., J. Vaynberg, X. Kong, T.A. Haas, E.F. Plow, and J. Qin. 2004. Membrane-mediated structural transitions at the cytoplasmic face during integrin activation. *Proc. Natl. Acad. Sci. USA.* 101:4094–4099.

Wennerberg, K., A. Armulik, T. Sakai, M. Karlsson, R. Fassler, E.M. Schaefer, D.F. Mosher, and S. Johansson. 2000. The cytoplasmic tyrosines of integrin subunit beta1 are involved in focal adhesion kinase activation. *Mol. Cell. Biol.* 20:5758–5765.

Zhang, H., J.S. Berg, Z. Li, Y. Wang, P. Lang, A.D. Sousa, A. Bhaskar, R.E. Cheney, and S. Stromblad. 2004. Myosin-X provides a motor-based link between integrins and the cytoskeleton. *Nat. Cell Biol.* 6:523–531.